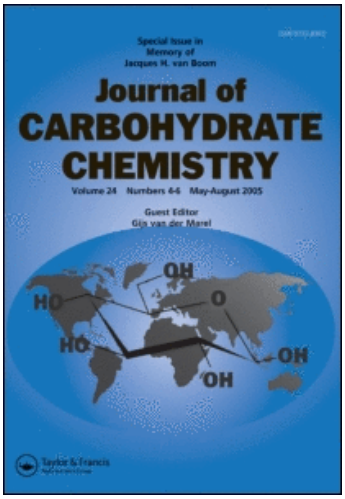

Journal of Carbohydrate Chemistry

Publication details, including instructions for authors and subscription information:
http://www.informaworld.com/smpp/title~content=t713617200

Bioinformatics Analysis of Oligosaccharide Phosphorylation Effect on the Stabilization of the β-Amylase Ligand Complex

Małgorzata Dudkiewicz[a]; Joanna Simińska[b]; Krzysztof Pawłowski[ac]; Sławomir Orzechowski[b]
[a] Department of Biometrics and Bioinformatics, Warsaw University of Life Sciences, Warsaw [b] Department of Biochemistry, Faculty of Agriculture and Biology, Warsaw University of Life Sciences, Warsaw [c] Nencki Institute of Experimental Biology, Warsaw

To cite this Article Dudkiewicz, Małgorzata , Simińska, Joanna , Pawłowski, Krzysztof and Orzechowski, Sławomir(2008) 'Bioinformatics Analysis of Oligosaccharide Phosphorylation Effect on the Stabilization of the β-Amylase Ligand Complex', Journal of Carbohydrate Chemistry, 27: 8, 479 — 495
To link to this Article: DOI: 10.1080/07328300802547863
URL: http://dx.doi.org/10.1080/07328300802547863

Journal of Carbohydrate Chemistry, 27:479–495, 2008

ISSN: 0732-8303 print / 1532-2327 online
DOI: 10.1080/07328300802547863

Bioinformatics Analysis of Oligosaccharide Phosphorylation Effect on the Stabilization of the β-Amylase Ligand Complex

Małgorzata Dudkiewicz,[1] Joanna Simińska,[2] Krzysztof Pawłowski,[3] and Sławomir Orzechowski[2]

[1]Department of Biometrics and Bioinformatics, Warsaw University of Life Sciences, 159 Nowoursynowska St., Building 37, 02-776 Warsaw
[2]Department of Biochemistry, Faculty of Agriculture and Biology, Warsaw University of Life Sciences, 159 Nowoursynowska St., Building 37, 02-776 Warsaw
[3]Department of Biometrics and Bioinformatics, Warsaw University of Life Sciences, 159 Nowoursynowska St., Building 37, 02-776 Warsaw; and Nencki Institute of Experimental Biology, 3 Pasteur St., 02-093 Warsaw

Starch is the most abundant storage carbohydrate produced in plants. The beginning of transitory starch degradation in plants depends mainly on day cycle, posttranslational regulation of enzyme activity, and starch phosphorylation, but the molecular mechanism of these factors' influence is not yet precisely described. The aim of our analysis was to investigate the effect of phosphorylation on the intermolecular energies for stabilization of the complexes between the set of phosphorylated and nonphosphorylated carbohydrate ligands and *Solanum tuberosum* (L.) β-amylase model. For performing protein-ligand docking procedures and calculating the binding energies, the DOCK6 and Glide 4.5 program suites were applied. We have observed simultaneously the effect of chain elongation, phosphorylation, and chain branching. Results of flexible ligand docking show that phosphorylation as well as chain elongation increase the stabilization of the ligand-protein complex.

Keywords Potato β-amylase catalytic site structure; Oligosaccharide phosphorylation

Received May 7, 2008; accepted October 11, 2008.
Address correspondence to Małgorzata Dudkiewicz, Department of Biometrics and Bioinformatics, Warsaw University of Life Sciences, 159 Nowoursynowska St., Building 37, 02-776 Warsaw, Poland. E-mail: malgorzata.dudkiewicz@omega.sggw.waw.pl

INTRODUCTION

Starch, besides sucrose, is one of the primary products of photosynthesis in leaves. The starch granule consists of two distinct polysaccharide types, amylose and amylopectin. Amylose is essentially a linear polymer of α-(1-4)-linked glucose chains, whereas amylopectin is a branched molecule; besides α-(1-4)–bonds it has also α-(1-6)–bonds between glucose moieties.[1] The chain length distribution and arrangement of the branch points within amylopectin allow the formation of organized arrays of closely packed left-handed double helices in the semicrystalline zones of the starch granule. Under normal conditions, all starch synthesized during daylight in chloroplasts is then degraded during the night. The observed periodical starch degradation at night could be divided into two periods: initiation of degradation and digestion of amylopectin and amylose into maltose, glucose, and maltotriose.[2,3] There are several important factors affecting rate of starch decomposition: circadian clock, gene regulation, starch phosphorylation, and regulation of enzyme activities. Native starch granule, as a semicrystalline structure, is an unfavorable substrate for most amylolytic enzymes.[4] For many years it was thought that α-amylases (EC 2.4.1.1) should start starch granule degradation in chloroplasts, but a later study has questioned this function of α-amylases.[5] Recently it was discovered that starch phosphorylation stimulates β-amylase (EC 2.4.1.2) activity.[6] Starch phosphorylation in *Arabidopsis* leaves is catalyzed by two dikinases—glucan, water dikinase GWD (EC 2.7.9.4), and phosphoglucan, water dikinase PWD/GWD3 (EC 2.7.9.5). Whereas GWD specifically phosphorylates the C6 position, PWD phosphorylates the C3 position of glucose moieties in the amylopectin molecule.[7] According to Blennow et al.,[8] there is some positive correlation between the chain length of the branched α-glucan and the amount of the phosphate covalently bound to it. Results obtained by Ritte et al.[9] prove that in the pool of short phosphorylated malto-oligosaccharides (DP7–DP23), isolated from potato leaf starch using isoamylase, single phosphorylated chains dominated. Double phosphorylated chains were longer than 16 DP.[9] In potato starch, most phosphate esters are bound in the C6 position (70%–80%), in contrast to the C3 position (20%–30%).[8,10] Detailed understanding in which way starch phosphorylation modulates β-amylase activity is still lacking. One possibility is that β-amylase and isoamylase 3 (EC 2.4.1.68) are not able to effectively attack the ordered, semicrystalline surface of the granule in chloroplast. The addition of phosphate groups to starch polymers may disrupt the organization of the granule matrix and make it a better substrate for exoamylolytic attack.[7,11,12]

β-Amylase is a specific 1,4-α-D-glucan maltohydrolase that catalyzes the hydrolysis of 1,4-α-glucosidic linkages in polysaccharides so as to remove successive maltose units from the nonreducing ends of the chains (Gene Ontology ID:GO 0016161). Substrates for β-amylase are oligosaccharide chains that are not branched and not phosphorylated as proposed by Edner et al.[6] β-amylase

is not able to pass 1,6-α-bonds nor by phosphates ester in the C6 or C3 position in the α-polyglucan chain. Moreover, maltose and cyclodextrin were reported to be inhibitors of the β-amylase reaction.[13,14]

In the beginning of this decade, there were some efforts of automated docking of different carbohydrate ligands to soybean β-amylase active site,[15,16] but without considering its phosphorylated forms. Starting from the 90-ties, a number of X-ray structures have been reported for plant and bacterial β-amylases, including the complexes with some oligosaccharides and inhibitors or artificial molecules as ligands.[13,17–20] The mechanisms of β-amylase hydrolysis of 1,4-α-glucosidic linkages in polysaccharides and the active site geometry, considering the key catalytic residues, were precisely described in 2004 by Akira et al.[18] and Kang et al.[13] Up to now there is no experimental structure for *Solanum tuberosum* β-amylase deposed in the databases, but the amino acid sequences for potato β-amylase are available in the GenBank (AAK84008.1, GI:15082058, PCT-BMYI).

We decided to examine the importance of starch phosphorylation for starch degradation process in potato, by studying the binding energies of several malto-oligosaccharides phosphorylated in C6 and C3 positions or nonphosphorylated, complexed with the structural model of the enzyme constructed for potato β-amylase amino acid sequence.

LIGAND PREPARATION

For obtaining detailed information on the influence of sugar chain elongation and branching on binding affinity to the β-amylase active site, we have collected experimentally resolved oligosaccharide structures available at the PDB site (Protein DataBank: http://www.rcsb.org/pdb/). Hence, we obtained maltose, maltotriose, maltotetraose, maltopentaose, and maltoheptaose ligands. Based on these structures, we have constructed two other potential substrates for β-amylase: malto-octaose and maltoheptaose with branched chain and 14 phosphorylated forms of oligosaccharides. A list of ligands that are potential

Table 1: The list of ligands (potential substrates for β-amylase) used in docking studies

Ligand	Molecular Formula
Maltotetraose	$C_{24}H_{42}O_{21}$
Phosphomaltotetraose	$C_{24}H_{43}O_{23}P$
Maltopentaose	$C_{30}H_{52}O_{26}$
Phosphomaltopentaose	$C_{30}H_{55}O_{29}P$
Maltoheptaose	$C_{42}H_{72}O_{36}$
Phosphomaltoheptaose	$C_{42}H_{75}O_{39}P$
Malto octaose	$C_{48}H_{88}O_{47}$
Phosphomaltooctaose	$C_{48}H_{87}O_{50}P$
Maltoheptaose branched	$C_{42}H_{72}O_{36}$
Phosphomaltoheptaose branched	$C_{42}H_{75}O_{39}P$

β-amylase substrates is presented in Table 1. All the ligands were next prepared for docking by adding hydrogens, charges (at pH 5.4), and energy minimization processes using UCSF Chimera[21,22] DockPrep applications for DOCK6 studies or Schrodinger LigPrep procedure for Glide 4.5 calculations. For constructing the phosphorylated variant for every ligand, we used a fixed phosphorylation pattern. Phosphate group was always introduced in the C6 or C3 position in the last glucose moiety at the reducing end of the carbohydrate chain. Finally, 21 molecular structures for potential ligands were gathered and prepared for docking process.

MODELING OF POTATO β-AMYLASE, STRUCTURE, AND RECEPTOR PREPARATION

Using the FFAS03 server, we chose two pdb entries: 1Q6C and 1BFN with the best score (-118.00, 46% of identity) as templates for homology modeling, containing, respectively, the crystal structure of soybean β-amylase complexed with maltose and the structure of soybean β-amylase crystallized without the ligand. The model of potato β-amylase PCT-BMYI (a homolog of *A. thaliana* sequence CT-BMY [β-amylase 8, BAM3, AT4G17090] with BLAST e-value 6.9e-217 and similarity of 83%) was constructed using the project mode of SWISS-MODEL, a fully automated comparative modeling server.[23–25] After automatic superposition of the template structures ("magic fit" tool of PDB SwissViewer) and fitting of raw amino acid sequence of potato β-amylase into the template using Deep Viewer, the modeling procedure performed by the server consisted of three standard steps: model building, structure minimization, and evaluation. The resulting structural alignment of PCT-BMYI and Q6C/BFN sequences is presented in Figure 1; the structure of the template protein (soybean β-amylase) is shown in Figure 2a and b.

According to crystallographic data,[18] the ligand binding site in β-amylase structure is situated in the β-sheet barrel surrounded by radially located α-helices. As determined by Akira et al.,[18] $Glu^{186}$and Glu^{380} play crucial roles in the enzymatic reaction as the main acid and base catalysts, respectively. Some other residues (Lys^{295}, Met^{51} and Asn^{340}, Glu^{178}, Gln^{87} and Asp^{176}) form a kind of hydrogen bond network that stabilizes the negative charge of Glu^{380}.

According to Akira et al.[18] the optimum pH for higher plant β-amylases is around 5.4. It has been also proven that reduced pKa value of Glu^{380}stabilized by the hydrogen bond network between the side chains of the residues mentioned is responsible for lower pH optimum of soybean β-amylase compared to that of the known bacterial ones.[13,18] Apart from the main catalytic residues, some conserved residues (from position 96 to 103) that build a flexible and moving loop play an important role in both the binding of the substrate and the releasing of the product in the case of soybean β-amylase. As can be seen

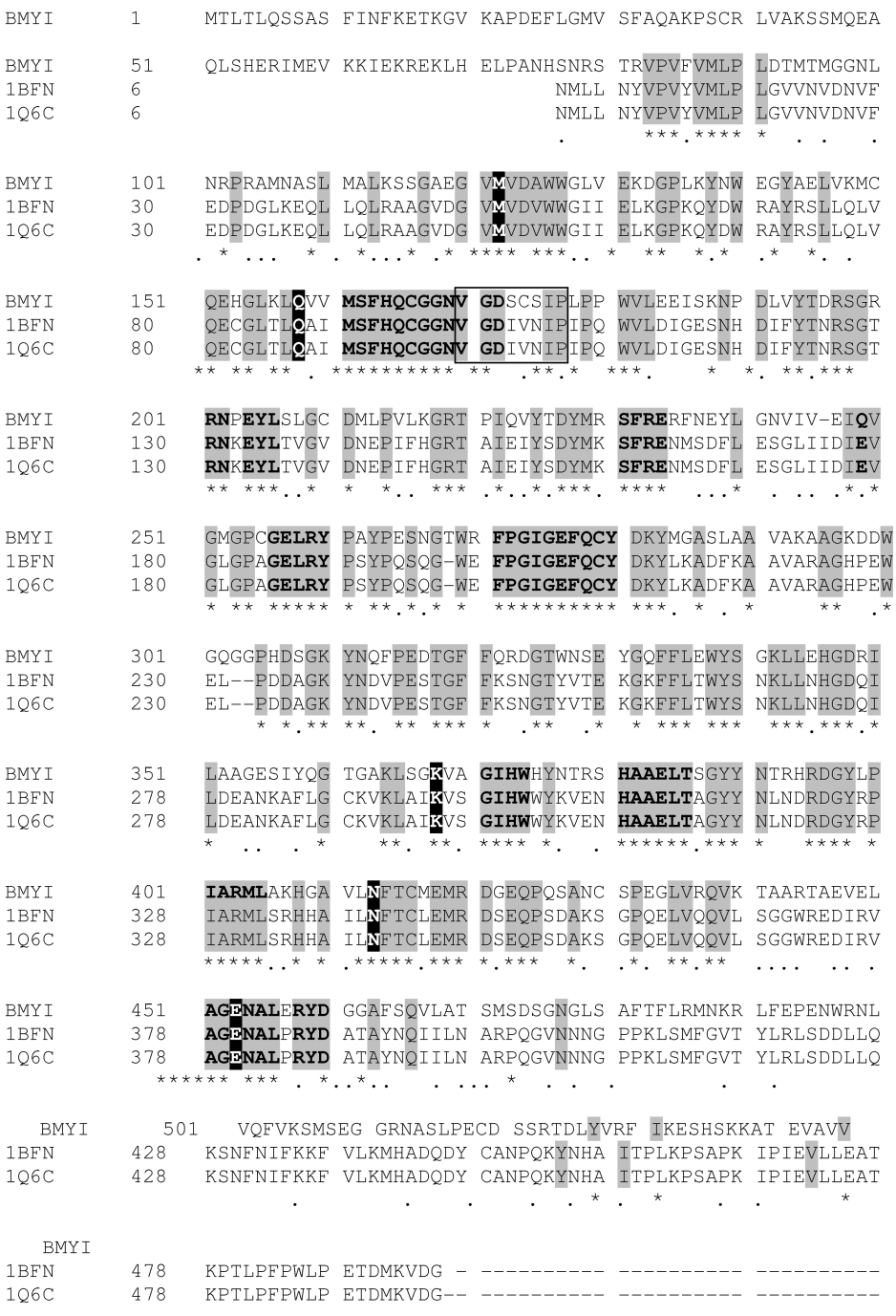

Figure 1: The structural alignment of PCT-BMYI and 1BFN/Q6C amino acid sequences. White bold residues represent the amino acid side chains responsible for creating the hydrogen bond network in the soybean β-amylase active site.

in Figure 1, all crucial residues of soybean β-amylase (except two last residues from moving loop) are conserved in the potato sequence.

The soybean β-amylase active site is described as an $(\alpha.\beta)_8$barrel core with five subsites for subsequent glucosyl units of oligosaccharide substrate.[13,15] The enzyme hydrolytic site is located between sites -1 and $+1$ where two highly conserved residues ($Glu^{380}$and Glu^{186}) are located. Basing on docking results, we made an effort to identify the binding subsites in the potato β-amylase model (Fig. 3) and to check the possibility of binding ligands longer than five glucosyl rings. Because of lacking suitable crystal structures of ligand–receptor complexes between potato β-amylase and oligosaccharide ligands, we could not perform structure comparisons, which should confirm obtained docking results. Proposed binding modes are thus purely hypothetical. As a kind of "sanity check," which we were able to perform, we have measured RMSD (root mean square deviation) for 1Q6C structure (soybean β-amylase and two maltose units in the binding site) and our model with docked maltotetraose. Overall RMSD was 0.43 A. The RMSD for the ligands only were

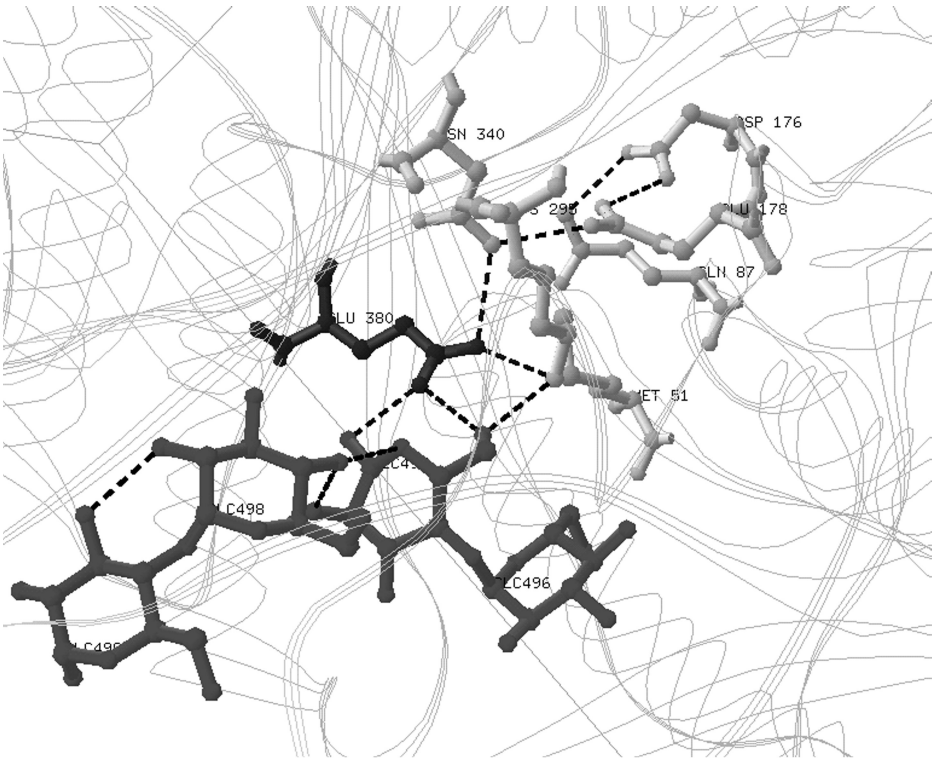

(a)

Figure 2: (a) Active site of soybean β-amylase with 2 maltose molecules as a ligand (source: 1Q6C.pdb) (b) hydrogen bonds network and the ligand in the β-amylase active site. *(Continued)*

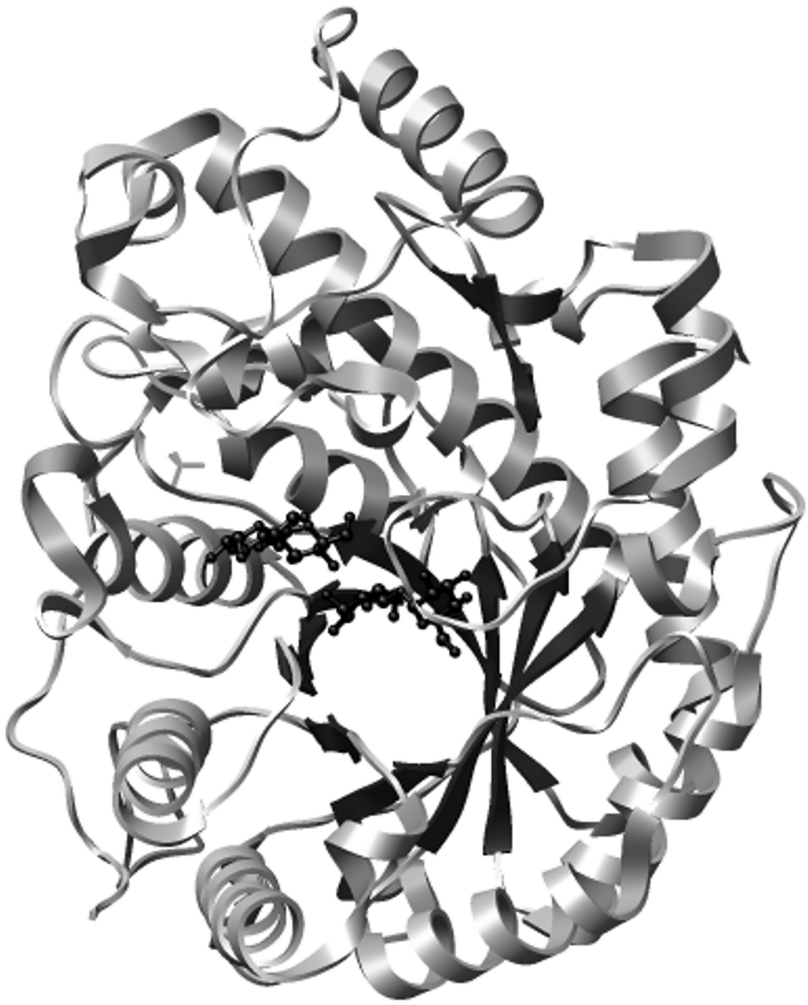

(b)

Figure 2: (Continued)

above 3.0 A, what could be caused by the fact that the crystal structure was crystallized with two maltose molecules, which are indeed the products, not the substrates, for β-amylases.

All docking studies were performed using the DOCK6[26] program suite and the MacroModel 7.0 software and partially, Glide 7.0 algorithms. DOCK6 was implemented for prepositioning of the big ligands within the active site region, which surface was approximated and simplified for calculation reasons using the dms[27,28] and sphgen[29] algorithms. As a DOCK6 suite graphical interface, UCSF Chimera (beta version 1)[22] and Swiss PDB Viewer were used. MacroModel 7.0 processes were run from Maestro GUI platform installed in the environment of Fedora Linux 7.0. DOCK6 calculations were performed on

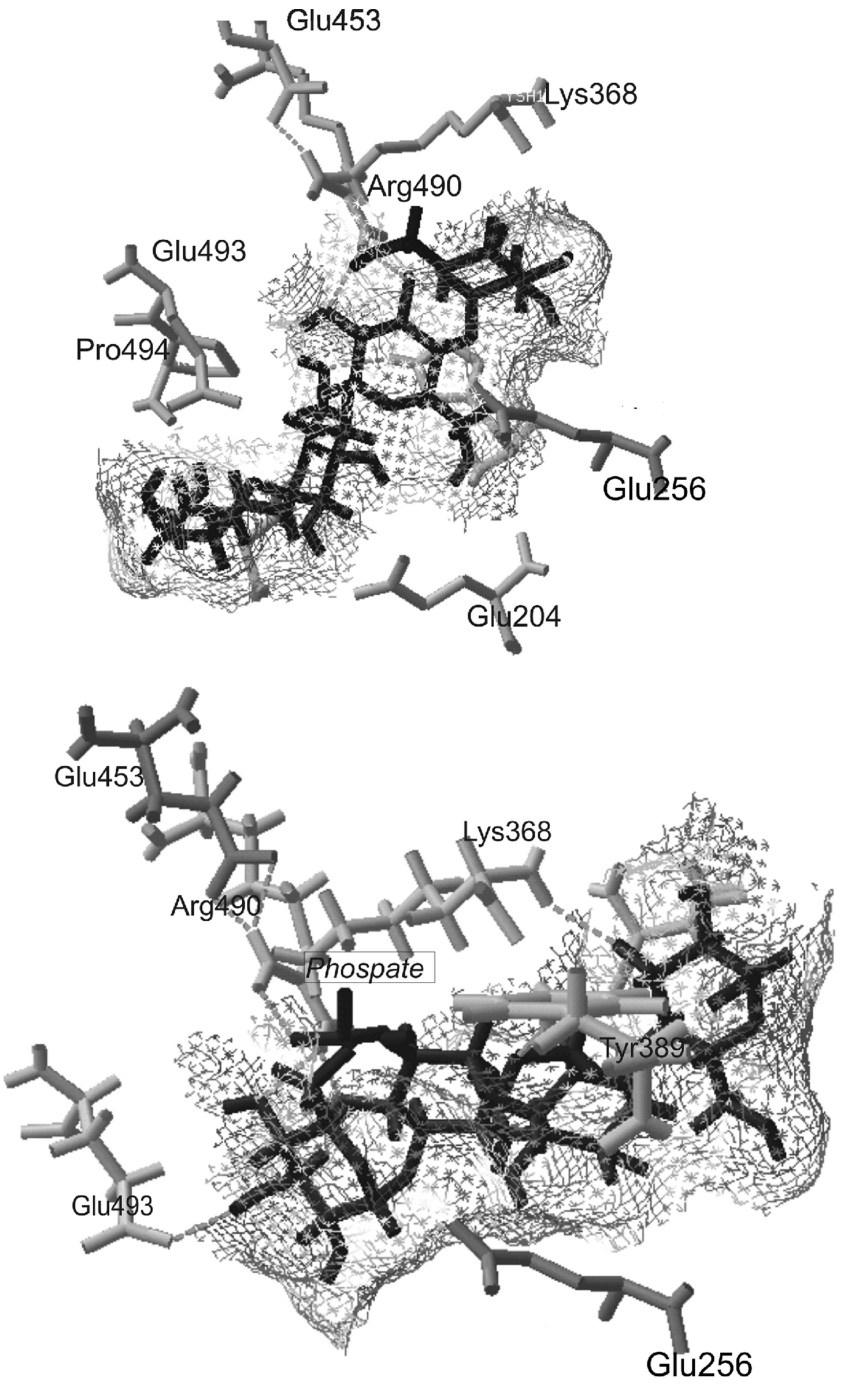

Figure 3: Differences in the lowest energy docking positions for maltotetraose (A) and C6 phosphomaltotetraose (B) at potato β-amylase active site. The residues surrounding the binding site and making hydrogen bonds with ligand are depicted grey, oligosaccharides are presented as black sticks with surface representation.

the cygwin platform at the cluster of 16 Windows PCs (2.8 GHz and 512 MB RAM) built using Condor 6.8.7 cluster managing software.

DOCKING STUDIES

For all of the flexible docking simulations using the DOCK6 program suite, the AMBER molecular mechanics force field was employed. In the case of reported studies only the interactions between the ligand and protein were considered. Since the receptor was considered rigid, the receptor contribution to the total potential energy was precalculated and the scoring grid was created. Force field scores are approximate molecular mechanic interaction energies, consisting of two components: intermolecular van der Waals (VDW) and electrostatics interactions, given by formula 1.1. The grid calculation was limited to the β-amylase active site (residues from 111 to 258 and from 349 to 469) determined using the structural alignment with the 1Q6C structure. This set of residues contained the hypothetical key catalysts: Met^{122}, Glu^{453}, Asn^{430}, and Lys^{368} and the potentially flexible loop corresponding to the ^{96}GGNVGDIV^{103} sequence from soybean β-amylase. Loop was modeled in closed conformation, which, according to Laederach et al.,[16] creates an environment more favorable for docking of soybean β-amylase. For flexible docking the "anchor-and-grow" conformational search algorithm was used.

$$E = \sum_{i=1}^{lig} \sum_{j=1}^{rec} \frac{A_{ij}}{r_{ij}^{a}} - \frac{B_{ij}}{r_{ij}^{b}} + 332 \frac{q_i q_j}{D r_{ij}} \tag{1.1}$$

Automated docking procedure was performed for ligands with less than 35 rotatable bonds and less than 200 atoms (including hydrogens) using Glide 4.5 software in flexible standard precision docking mode with automatic generation of conformations for each input ligand. Glide (Grid-based Ligand Docking with Energetics) searches for favorable interactions between the receptor (a protein) and the molecules supposed to be ligands were performed. After generating a number of possible ligand orientations, the program evaluated the interactions of each of them with the receptor. The best poses entered the final step of the algorithm, which was energy minimization of the ligand-receptor complex involving the OPLS-AA force field energy grid. Final scoring using Glide Score function was carried out on energy-minimized poses. The ligand positions obtained were then ranked using the Glide Score values (elements that make up the GScore function are specified under Table 2).

RESULTS AND DISCUSSION

We obtained a series of DOCK6 docking energy scores in kcal/mol (see Table 3 and Fig. 4) and a more complex measure of docking energy, called Glide Score, from Glide 4.5 (Table 2). There is a remarkable trend in the ligand

Table 2: Results for the six ligand-receptor pairs (β-amylase and maltose, maltotriose, and maltotetraose and its phosphorylated forms) obtained using Glide 4.5 software with OPLS-AA force field (calculation for ligands longer than four glucose rings could not be performed because of the program internal limitation for the number of atoms and rotatable bond for ligand molecules)

Rank of the ligand		Score	Lipo	H Bond	Rewards	vdW	Coul	RotB
1	phosphomaltotetraose	−6.37	−0.2	−0.7	−0.1	−38.0	−28.5	0.2
2	phosphomaltotriose	−6.33	−0.1	−1.5	0.0	−27.6	−39.1	0.4
3	maltose	−6.28	−0.1	−1.2	−1.0	−25.2	−27.6	0.6
4	maltotetraose	−5.80	−1.1	−0.2	−0.5	−30.9	−20.2	0.3
5	maltotriose	−5.73	−1.0	−0.3	−0.5	−31.6	−20.6	0.5
6	phosphomaltose	−4.34	0.0	−1.2	−0.5	−17.8	−20.3	0.6

		Site	E model	CvdW	Intern	Conf	# Pose#
1	phosphomaltotetraose	0.1	−86.6	−66.5	20.2	92	364
2	phosphomaltotriose	0.6	−87.3	−66.7	21.4	139	102
3	maltose	0.3	−69.6	−52.7	19.7	23	62
4	maltotetraose	0.1	−57.0	−51.1	17.5	197	317
5	maltotriose	0.0	−67.4	−52.2	11.1	131	53
6	phosphomaltose	0.4	−51.0	−38.1	4.9	120	384

Final score is a combination of a set of indices, for comparison with DOCK6 score only CvdW parameter (the nonbonded interaction energy between the ligand and the receptor) should be considered. Units: kcal/mol.
GlideScore (GScore) = a * vdW + b * Coul + Lipo + Hbond + Metal + Rewards + RotB + Site + Emodel + CvdW,
where: vdW = van der Waals interaction energy
Coul = coulomb interaction energy
Lipo = lipophilic-contact plus phobic-attractive term
H Bond = hydrogen-bonding term
Rewards = various reward or penalty terms
RotB = penalty for freezing rotatable bonds
Site = Polar interactions in the active site, and the coefficients of vdW and Coul are: a = 0.063, b = 0.120 for Standard Precision (SP), Glide 4.5. CvdW = Coul + vdW is the nonbonded interaction energy between the ligand and the receptor. E model is a specific combination of GScore, CvdW, and Intern, which is the internal torsional energy of the ligand conformer.

docking energy. Generally, for longer polymers we observed an increase in binding affinities, but for branched ones there was a switch in trend or even a decrease stated. The influence of glucose moiety phosphorylation was noted in DOCK6 as well as in Glide 4.5 calculations. We have not repeated the calculations done for ligands longer than four glucose residues using Glide 4.5 because of internal limitations of the automated docking procedure, which excluded longer ligands. Obtained results were obviously different with regard to the absolute values but comparable regarding ligand ranking (in the range of 2DP to 4DP within which we were able to make comparison of docking methods). Energies obtained from DOCK6 calculations were similar in range with ligand-receptor interaction energies reported by Laederach et al.[16] for docking of various oligosaccharide ligands into the active site of crystal structure of soybean β-amylase. The correlation between intermolecular energy values obtained by Laederach et al.[16] and the results received from DOCK6 calculation for maltose, maltotriose (not shown in Table 3), and maltotetraose is very high ($r = 0.98$). For DOCK6 and Glide 4.5 results (for the same ligands), the correlation is not so significant ($r = 0.81$). The energies of stabilization for the complexes

Table 3: Results of DOCK6 calculations with AMBER force field obtained for 12 ligand-receptor pairs.

C6	phosphomaltotetraose	phosphomaltopentaose	phosphomaltoheptaose	Phosphomalto-octaose	Phosphomaltoheptaose (branched form)
Dock Score	−101.4	−105.3	−111.8	−131.4	−114.4
VdW	−62.6	−72.2	−75.5	−98.5	−84.5
ES	−38.8	−33.0	−36.3	−32.4	−29.9
C3	**phosphomaltotetraose**	**phosphomaltopentaose**	**phosphomaltoheptaose**	**phosphomalto-octaose**	**phosphomaltoheptaose (branched form)**
Dock Score	−93.7	−103.7	−130.6	−144.6	−112.6
VdW	−61.4	−75.0	−99.6	−114.2	−75.0
ES	−32.3	−28.7	−31.0	−30.4	−37.6
	maltotetraose	**maltopentaose**	**maltoheptaose**	**malto-octaose**	**maltoheptaose (branched form)**
Dock Score	−78.1	−92.9	−118.6	−137.7	−131.8
VdW	−52.5	−69.8	−92.3	−106.1	−93.8
ES	−25.6	−23.1	−26.2	−31.6	−37.9

VdW is van der Waals energy component, ES is electrostatic interaction energy. Final score (DOCK Score) is a sum of these two components and could be compared with the CvdW parameter from Table 3. Units: kcal/mol.

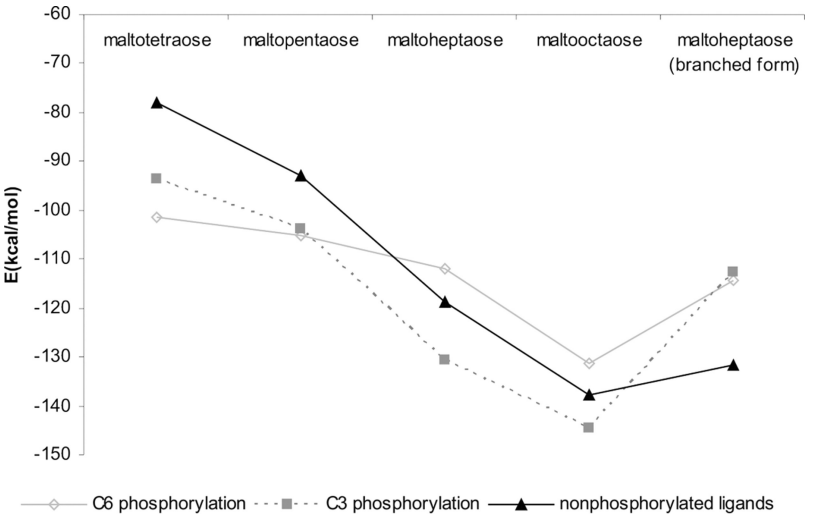

Figure 4: The influence of the phosphorylation (in C6 and C3 positions, respectively) of the glucose ring of five tested oligosaccharides on the docking energy. The black solid line connects the energy points (black diamonds) for nonphosphorylated ligands, the gray diamonds connected by the gray solid line represent C6 phosphorylated ligands, and the gray squares connected by the gray dotted lines represent C3 phosphorylation products. Results of subsequent DOCK6 run with AMBER force field.

of the β-amylase with the phosphorylated forms of maltose, maltotriose, and maltotetraose, calculated during the DOCK6 runs, were even up to 75% higher than for nonphosphorylated forms of the same oligosaccharides. These differences were relatively smaller in Glide calculations (Table 2), but still phosphorylated forms of maltotriose and maltotetraose turned out better candidates for binding in the β-amylase active site. For maltoheptaose and malto-octaose, we observed the opposite tendency: phosphorylation in C6 slightly decreased the binding energy of these oligosaccharides and remarkably reduced the binding propensity in the case of the branched oligosaccharide with phosphate groups introduced in C6 as well as in C3. In the case of C3 phosphorylation, this decrease in binding energy for linear ligands was not observed (see Fig. 4). In Figure 5, we compare best scoring docking poses for C6 phosphorylated and nonphosphorylated malto-octaose. C6 phosphomalto-octaose is docked in the characteristic position, in which the phosphate group sticks out from the binding site pocket, while the structure of the rest of the molecule seems to be more relaxed than the maltooctaose molecule in its best docking position (Figure 5). A different situation was observed for maltotetraose and its C6 phosphorylated equivalent. The orthophosphate group creates hydrogen bonds with arginine and lysine side chains, which could be responsible for the visible shift toward the tyrosine and valine residues enabling the new interactions between the receptor and the ligand (Fig. 3 and Table 4). The binding energy is bigger but the influence on the catalytic reaction could be quite opposite, because the

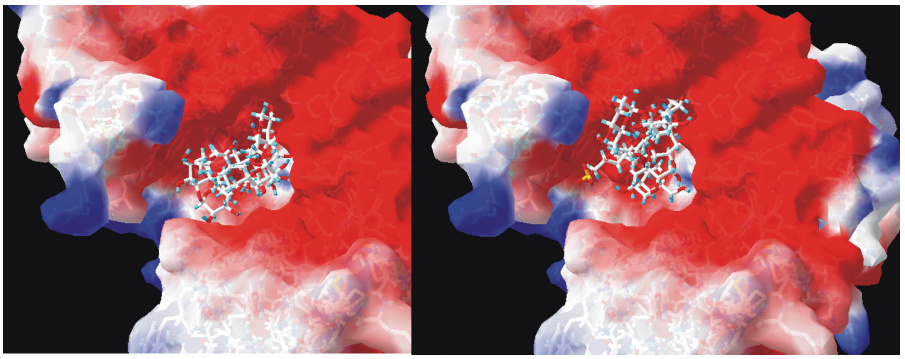

Figure 5: Comparison of the best scoring ligand poses obtained from DOCK 6 run for maltooctaose (A) and its C6 phosphorylated form (B). The receptor is shown in surface representation coloured according to electrostatic potential in red-blue traditional scale and the ligands molecules are presented in ball-and-stick model in CPK colour scheme.

phosphate group could block the interaction between the potential catalyst residue Glu^{453} and the attacking water molecule, which should enter the cleft in the way, enabling the interaction with C1 of the glucosyl unit in the subsite −1.

Analysis of docking energy components obtained from DOCK6 calculations revealed that the electrostatic part of interaction energy is rather stable or even decreases for longer phosphorylated ligands, while for nonphosphorylated ones electrostatic energy of the complex increases with the chain elongation. In the case of nonphosphorylated ligands as well as for phosphorylated oligosaccharides, Van der Waals forces are responsible for the overall shape of the energy plot (Fig. 4).

As proposed by Zeeman et al.[3] and Samojedny and Orzechowski,[2] starch phosphorylation occurs before the starch breakdown starts. The general role of phosphorylation (without discrimination in C3 or C6 positions) is still under debate, but the most common hypothesis claims that phosphorylation

Table 4: Proposed subsites for glucosyl units of potential oligosaccharides ligands in potato β-amylase active site

Subsites	Residues	Number of glucosyl units of maltotetraose	Number of glucosyl units of phosphomaltotetraose
−3	Glu493, Glu204, Pro494	1 (first from reducing end)	
−2	Glu493, His264	2	1 (first from reducing end)
−1	Glu256, Glu453, Arg490	3	2 (P)
+1	Arg490	(first from nonreducing end)	3
+2	Tyr389, Lys368, Val249		4 (first from nonreducing end)

(P), phosphate group at the C6 of glucosyl unit #1.

increases the exposure of amylopectin chains to amylolytic attacks.[6] The observed increased binding capacities of linear and phosphorylated ligands in the C3 position in our docking studies suggest that starch phosphorylation as a result of PWD activity could be a necessary initiating step in the starch degradation process, at least in potato. However in *Arabidopsis* leaves without prephosphorylation of starch granule catalyzed by GWD, PWD remains inactive.[11] In contrast to linear oligosaccharides, phosphorylation both in the C6 and C3 position of branched maltoheptaose seems to have similar influence on the binding energy of carbohydrate ligands to the active site of β-amylase.

A decrease of binding affinity in the cases of branched and phosphorylated longer carbohydrate ligands could be easily explained: β-amylase hydrolyzes each second an α-1,4 glycolytic bond starting from the nonreducing end of the α-glucans, but this enzyme is not able to pass through an α-1,6 glycolytic bond, which must be cleaved by isoamylase. Also, phosphorylation at the nonreducing end of the substrate, in contrast to the case of SBE (starch branching enzyme-EC 2.4.1.18) activity, inhibits β-amylase.[6,30]

As the number of substrate binding subsites in the potato β-amylase active site is probably similar to the number of subsites in its soybean homolog, it is expected that ligands longer than five glucosyl units can demonstrate lower binding affinities to the ligand binding cleft. On the other side, longer oligosaccharides may enter in the cleft in more packed conformation, which could be relatively stable (see docking results for maltoheptaose, Fig. 6). The phosphate group at the reducing end can act as an anchor, which does not allow longer ligands to bind in unfavorable conformation.

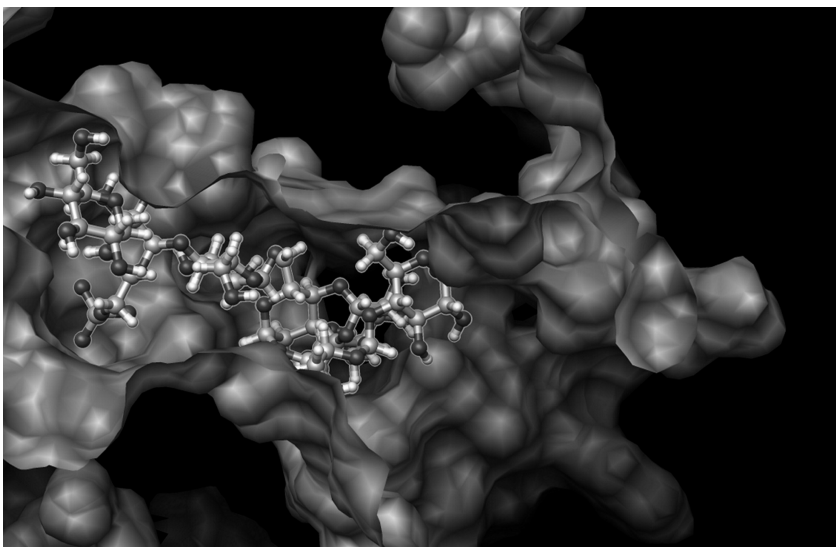

Figure 6: Branched form of C6 phosphomaltoheptaose in the active site of β-amylase – ligand is colored by CPK scheme.

In order to analyze better the influence of phosphorylation of possible β-amylase substrates on their binding affinity, we constructed the molecular surface of the enzyme and colored it by electrostatic potential in red-blue scale. We observed a characteristic pattern. The surface of the active site neighborhood is composed mostly of negatively charged residues; only on the bottom of the cleft, amino acids with positively charged side chains are found. Additionally, a group of positively charged side chains closes the binding cleft from the outside.

Figure 5 presents the comparison of the best scoring poses for maltooctaose and its C6 phosphorylated form with regard to the receptor surface electrostatic potential. C6 phosphomaltooctaose is shifted toward the positively charged part of the β-amylase molecule and the phosphate group remains at the outside of the binding pocket, probably interacting with the group of positively charged residues at its entrance. In the case of C6 phosphomaltotetraose and smaller ligands, we observed the opposite situation; the phosphate group very precisely entered the positively charged pocket in the middle of the active site.

CONCLUSION

Phosphorylation of short carbohydrate ligands both in the C3 and C6 positions influences its ability to bind to potato β-amylase. Phosphorylation in the C3 position in linear maltooligosaccharides enhances docking energy compared to the nonphosphorylated ligands. Taken together with postulated structure changes of starch granule, it may be sufficient for initiation of native starch breakdown. Obtained docking scores are in agreement with recently reported results of Edner et al.,[6] which explains activation of β-amylase in *Arabidopsis* due to starch phosphorylation. However, our bioinformatics study should be confirmed by crystallographic analysis.

ACKNOWLEDGMENTS

The authors thank the Polish Ministry of Science and Higher Education for financial support (Grant no. N302061134 to K.P. and S.O.).

REFERENCES

1. Hizukuri, S. Polymodal distribution of the chain lengths of amylopectin, and its significance Carbohydr. Res. **1986**, *147*, 342–347.

2. Samojedny, D.; Orzechowski S. New look at starch degradation in *Arabidopsis thaliana* L. chloroplasts. Post. Biochem. **2007**, *53*, 74–83.

3. Zeeman, S.C.; Delatte, T.; Messerli, G.; Umhang, M.; Stettler, M.; Mettler, T.; Steb, S.; Reinhold, H.; Kötting O. Starch breakdown: recent discoveries suggest distinct pathways and novel mechanisms. Functional Plant Biol. **2007**, *34*, 465–473.

4. Tester, R.F.; Karkalas, J.; QI, X. Starch structure and digestibility: enzyme-structure relationship. World's Poultry Sci. J. **2004**, *60*, 186–195.

5. Yu, T.S.; Zeeman, S.C.; Thorneycroft, D.; Fulton, D.C.; Dunstan, H.; Lue, W.L.; Hegemann, B.; Tung, S.Y.; Umemoto, T.; Chapple, A.; Tsai, D.L.; Wang, S.M.; Smith, A.M.; Chen, J.; Smith, S.M. Alpha-amylase is not required for breakdown of transitory starch in *Arabidopsis* leaves. J Biol Chem. **2005**, *280*, 9773–9779.

6. Edner, Ch.; Li, J.; Albrecht, T.; Mahlow, S.; Hejazi, M.; Hussain, H.; Kaplan, F.; Guy, Ch.; Smith, S.M.; Steup, M.; Ritte, G. Water dikinase activity stimulates breakdown of starch granules by plastidial β-amylases. Plant Physiol. **2007**, *145*, 17–28.

7. Ritte, G.; Heydenreich, M.; Mahlow, S.; Haebel, S.; Kotting, O.; Steup, M. Phosphorylation of C6- and C3-positions of glucosyl residues in starch is catalysed by distinct dikinases. FEBS Lett. **2006**, *580*, 4872–4876.

8. Blennow, A.; Bay-Smidt, A.M.; Olsen, C.E.; Moller, B.L. The distribution of covalently bound phosphate in the starch granule in relation to starch crystallinity. Int J Biol. Macromol. **2000**, *27*, 211–218.

9. Ritte, G., Scharf, A., Eckermann, N., Haebel, S., Steup, M. Phosphorylation of transitory starch is increased during degradation. Plant Physiol. **2004**, *135*, 2068–2077.

10. Tabata, S., Hizukuri, S. Studies on starch phosphate. Part 2. Isolation of glucose-3-phosphate and maltose phosphate by acid hydrolysis of potato starch. Starch **1971**, *23*, 267–272.

11. Kötting, O.; Pusch, K.; Tiessen, A.; Geigenberger, P.; Steup, M.; Ritte, G. Identification of a novel enzyme required for starch metabolism in *Arabidopsis* leaves. The phosphoglucan, water dikinase. Plant Physiol. **2005**, *137*, 242–252.

12. Engelsen, S.B.; Madsen, A.; Blennow, A.; Motawia, M.S.; Møller, B.L.; Larsen, S. The phosphorylation site in double helical amylopectin as investigated by a combined approach using chemical synthesis, crystallography and molecular modelling. FEBS Lett. **2003**, *541*, 137–144.

13. Kang, Y.N; Adachi, M.; Utsumi, S.; Mikami, B. The roles of Glu186 and Glu380 in the catalytic reaction of soybean β-amylase. J. Mol. Biol. **2004**, *339*, 1129–1140.

14. Thoma, J.A.; Koshland, D.E. Competitive inhibition by substrate during enzyme action. Evidence for induced-fit theory. J. Am. Chem. Soc. **1960**, *82*, 3329–3333.

15. Rockey, W.M.; Laederach, A.; Reilly, P. Automated docking of alpha-(1→4)-and alpha-(1→6)-linked glucosyl trisaccharides and maltopentaose into the soybean beta-amylase active site. J. Proteins **2000**, *40*, 299–309.

16. Laederach, A.; Dowd, M.K.; Coutinho, P.M.; Reilly, P.J. Automated docking of maltose, 2-deoxymaltose, and maltotetraose into the soybean beta-amylase active site. Proteins **1999**, *37*, 166–175.

17. Adachi, M.; Mikami, B.; Katsube, T.; Utsumi, S. Crystal structure of recombinant soybean beta-amylase complexed with beta-cyclodextrin. J. Biol. Chem. **1998**, *273*, 19859–19865.

18. Akira, H.; Adachi, M.; Atsushi, S.; Kang, Y.N.; Shigeru, U.; Bunzo, M. Structural and enzymatic analysis of soybean β-amylase mutants with increased pH optimum. J. Biol. Chem. **2004**, *279*, 7282–7295.

19. Oyama, T.; Miyake, H.; Kusunoki, M.; Nitta Y. Crystal structures of β-amylase from *Bacillus cereus* var. *mycoides* in complexes with substrate analogs and affinity-labeling reagents. J. Biochem. **2003**, *133*, 467–474.

20. Ye, Z.; Miyake, H.; Tatsumi, M.; Nishimura, S.; Nitta Y. Two additional carbohydrate-binding sites of ß-amylase from *Bacillus cereus* var. *mycoides* are involved in hydrolysis and raw starch-binding. J. Biochem. **2004**, *135*, 355–363.

21. Pettersen, E.F.; Goddard, T.D.; Huang, C.C.; Couch, G.S.; Greenblatt, D.M.; Meng, E.C.; Ferrin, T.E. UCSF chimera - a visualization system for exploratory research and analysis. J. Comput. Chem. **2004**, *25*, 1605–1612.

22. Meng, E.C.; Pettersen, E.F.; Couch, G.S.; Huang, C.C.; Ferrin, T.E. Tools for integrated sequence-structure analysis with UCSF Chimera. BMC Bioinformatics **2006**, *7*, 339.

23. Schwede, T.; Diemand, A.; Guex, N.; Peitsch, M.C. Protein structure computing in the genomic era. Res. Microbiol. **2000**, *151*, 107–112.

24. Schwede, T.; Kopp, J.; Guex, N.; Peitsch, M.C. SWISS-MODEL: an automated protein homology-modeling server. Nucl. Acids Res. **2003**, *31*, 3381–3385.

25. Peitsch, M.C.; Schwede, T.; Guex, N. Automated protein modelling—the proteome in 3D. Pharmacogenomics **2000**, *1*, 257–266.

26. Moustakas, D.T.; Lang, T.; Pegg, S.; Pettersen, E.; Kuntz, I.D.; Brooijamans, N.; Rizzo, R.C. Development and validation of a modular, extensible docking program: DOCK 5. J. Comput. Aided Mol. Des. **2006**, *20*, 601–619.

27. Richards, F.M. Areas, volumes, packing, and protein structure. Ann. Rev. Biophys. Bioeng. **1977**, *6*, 151–176.

28. Connolly, M. Protein surfaces and interiors. Ph.D. Thesis, University of California, Berkeley, 1981.

29. Kuntz, I.D.; Blaney, J.M.; Oatley, S.J.; Langridge, R.; Ferrin, T.E. A geometric approach to macromolecule-ligand interactions. J. Mol. Biol. **1982**, *161*, 269–288.

30. Viksø-Nielsen, A.; Blennow, A.; Nielsen, T.H; Møller, B.L. Phosphorylated α(1,4) glucans as substrate for potato starch-branching enzyme. Plant Physiol. **1998**, *117*, 869–875.